Synthesis, Pharmacological Evaluation, and Molecular Modeling Studies of Novel Peptidic CAAX Analogues as Farnesyl-Protein-Transferase Inhibitors

Vincenzo Santagada,[†] Giuseppe Caliendo,[†] Beatrice Severino,[†] Antonio Lavecchia,[†] Elisa Perissutti,[†] Ferdinando Fiorino,[†] Angela Zampella,[‡] Valentina Sepe,[‡] Daniela Califano,[§] Giovanni Santelli,[§] and Ettore Novellino*[,†]

Dipartimento di Chimica Farmaceutica e Tossicologica, Università di Napoli ≪Federico II≫ Via D. Montesano 49, 80131 Napoli, Italy, Dipartimento di Chimica delle Sostanze Naturali, Università di Napoli ≪Federico II≫ Via D. Montesano 49, 80131 Napoli, Italy, and Dipartimento di Oncologia Sperimentale, Istituto dei Tumori ≪Fondazione Pascale≫, via Semmola 80131, Napoli, Italy

Received June 29, 2005

Fifteen analogues of the *C*-terminal CA_1A_2X motif were synthesized and evaluated for their inhibition potency against farnesyltransferase (FTase). Replacement of the A_2 residue by phenylalanine or tyrosine-derived analogues, in which a different number of methyl groups were introduced on the aromatic ring, resulted in compounds less active than the reference compound CVFM against FTase except for compounds **I** and **VI** (IC_{50} = 1 μM and 2.5 μM, respectively) that were comparable to CVFM and compound **IV** (IC_{50} = 0.1 μM), which was 6-fold more active than the reference compound. Because pseudopeptidic derivatives **I**−**IX** were inactive in the cellular assays, the *N*-formyl- and methyl-ester derivatives (compounds **X**−**XV**) were synthesized and tested on different cell lines, showing, in some cases, activity and appreciable selectivity against transformed cells. To rationalize the obtained results, molecular modeling experiments were carried out suggesting the molecular basis of FTase inhibition by these products.

Introduction

Although advances in medical science have greatly reduced the toll of many human diseases, cancer still presents challenges to effective treatment. Many signal transduction proteins, involved in cell growth and differentiation, have been identified as possible targets to develop new anticancer treatments.[1] One of the most studied proteins is Ras, a small GTP-binding protein that is an important switch in signal-transduction pathways that mediate growth-factor-stimulated cell proliferation.[2] Ras proteins are found mutated in 30−40% of all human cancers, and the mutation persistently causes a constitutive activation of the proteins that bind GTP. The three mammalian *ras* genes yield four Ras proteins: H-Ras, N-Ras, K-Ras4A, and K-Ras4B. Several evidences indicate that these different isoforms serve distinct functions. In this context, a very important aspect is that cancers arising in different organs are most often associated exclusively with a mutation in only one *ras* gene.[3] The attachment of an isoprenoid lipid (prenylation) to the *C*-terminus is the first and essential step in a series of posttranslational modification events that lead to the mature and activated Ras. Proteins farnesyltransferase (FTase) and geranyl-geranyltransferase (GGTase), collectively known as CAAX prenyltransferase, attach their isoprenoid groups, farnesyl and geranylgeranyl, to the *C*-terminal cysteine of the Ras and the Rab families of proteins, respectively.[4] Farnesylation is usually followed by additional modifications of the prenylated protein, such as the proteolytic removal of the last three residues of the CAAX box and the carboxymethylation of the new *C*-terminal-farnesylated cysteine.[5] Farnesylation is required for the subcellular localization and tranformation activity of the oncogenic variants of Ras. Consequently, the inhibition of isoprenylation prevents localization at the cell membrane, thereby prohibiting cell transformation; for this reason, the development of farnesyltransferase inhibitors, a novel approach to noncytotoxic anticancer therapy, has been an active area of research over the past decade.

Enzymatic and crystallographic techniques have explained the mechanistic details of FTase catalysis, demonstrating that farnesylation proceeds via an ordered mechanism with farnesyl pyrophosphate (FPP) binding first, followed by the CA_1A_2X substrate (where C is cysteine, A_1 and A_2 are aliphatic amino acids, and X is preferably serine or methionine), and then the cysteine of CA_1A_2X is farnesylated by the enzyme. During the search for farnesyltransferase inhibitors some simple tetrapeptides, based on CA_1A_2X, have shown to be able to work as substrate-analogue inhibitors of FTase, initiating a lot of research activity. It has been demonstrated that the introduction of an aromatic residue at the A_2 position has a positive effect on inhibitory potency against the enzyme, as exemplified by CVFM, CVWM, and CVYM, used as basis for further studies.[6] These compounds were found to be very interesting because of their capability to bind the FTase without being the substrate for the enzyme. The analysis of their ternary complexes suggested that the aromatic rings of the peptidic inhibitors did not allow the access of FPP to the binding site, preventing the farnesylation of these peptidic inhibitors and that there might be space for an additional hydrophobic interaction by the side chain of A_2 into the FPP binding site.[7] In an effort to further develop structure−activity relationships, in this article, we describe the synthesis and the biological activity of a third series[8] of nonsubstrate-tetrapeptidic inhibitors (CVFM and CVYM), where the aromatic residue in the A_2 position has been replaced with uncoded amino acids,[9] such as (2S,3aS,7aS)-octahydroindole-2-carboxylic acid (Oic),[10] 2′,4′-dimethylphenylalanine, 2′,3′-dimethyltyrosine, 2′,5′-dimethyltyrosine, and 2′-methyltyrosine, to improve the chemical stability of the resulting compounds and verify the possibility of additional hydrophobic interactions with the FTase binding site (Chart 1). Moreover, a molecular modeling study highlighted the site specificity and the inhibition mechanism for the examined derivatives.

* To whom correspondence should be addressed. Tel: 0039+81678643. Fax: 0039+81678649. E-mail: novellin@unina.it.

[†] Dipartimento di Chimica Farmaceutica e Tossicologica, Università di Napoli.

[‡] Dipartimento di Chimica delle Sostanze Naturali, Università di Napoli.

[§] Dipartimento di Oncologia Sperimentale.

10.1021/jm0506165 CCC: $33.50
Published on Web 02/24/2006

Chart 1. General Structures of the Synthesized Compounds

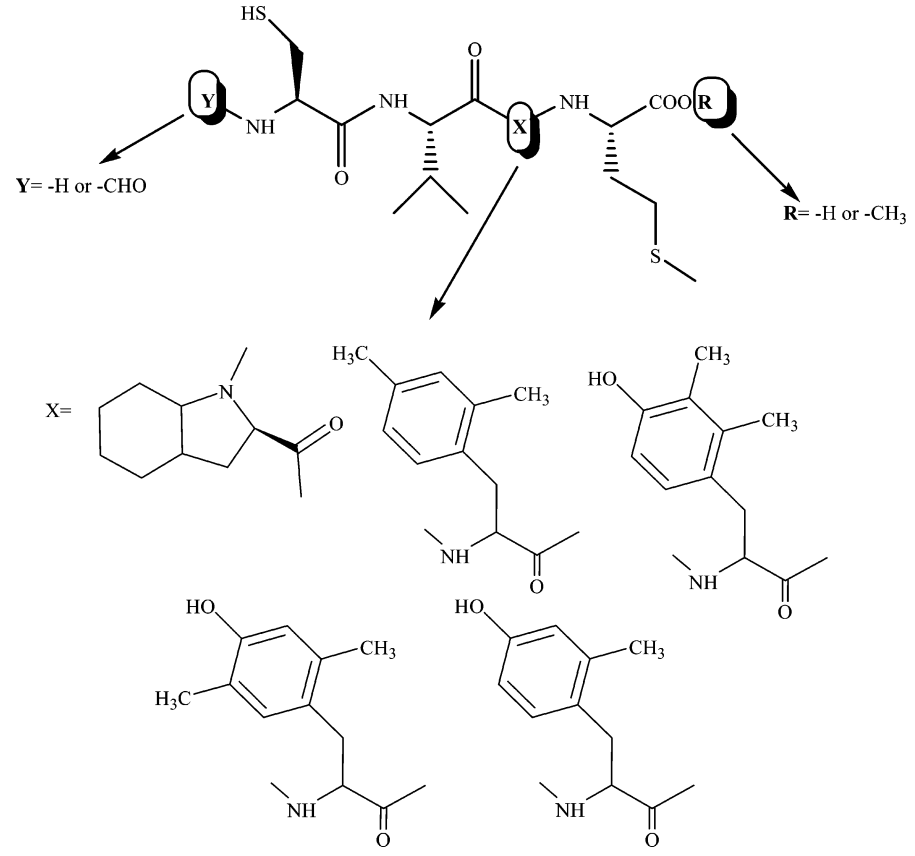

Scheme 1. Synthesis of the Unnatural Amino Acids (**1f**−**4f**)[a]

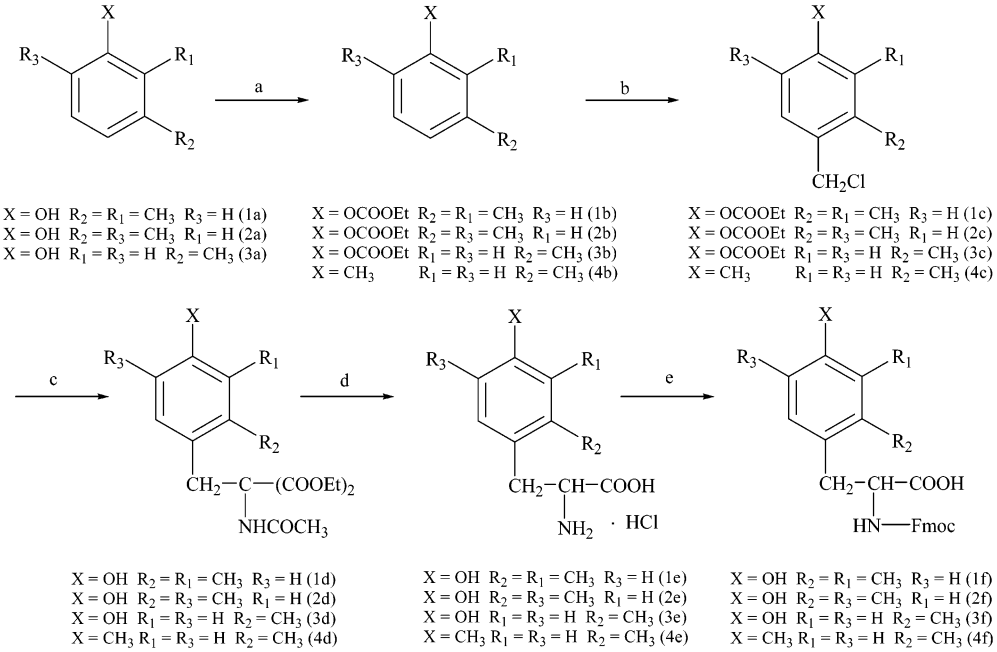

[a] Reagents and conditions: (a) ClCOOEt, pyridine; (b) CH_2O in concentrated HCl; (c) $CH_3CONHCH(COOEt)_2$ in EtOH/Na; (d) 6N HCl under reflux; (e) Fmoc−OSu, $NaHCO_3$ in dioxane.

Chemistry

Oic was prepared according to the procedure of Vincent et al.;[10] 2′,4′-dimethylphenylalanine (Dmp), 2′,3′-dimethyltyrosine (2,3-Dmt), 2′,5′-dimethyltyrosine (2,5-Dmt), 2′-methyltyrosine, as racemic mixtures, were prepared according to the method of Abrash et al. ad hoc modified and summarized in Scheme 1.[9]

The starting materials (**1a**−**3a**) were reacted with ethyl chlorocarbonate to obtain the corresponding *O*-carbethoxy intermediates (**1b**−**3b**). The chloromethylation of the *O*-carbethoxy derivatives (**1b**−**3b**) by CH_2O/HCl always gave the 4-chloromethyl derivatives (**1c**, **2c**, and **3c**). In addition, when chloromethylation was applied to *m*-xylene (**4b**), we obtained the derivative 2,4-dimethylbenzyl chloride (**4c**). Intermediates

Scheme 2. Synthesis of Compounds **XIV** and **XV**

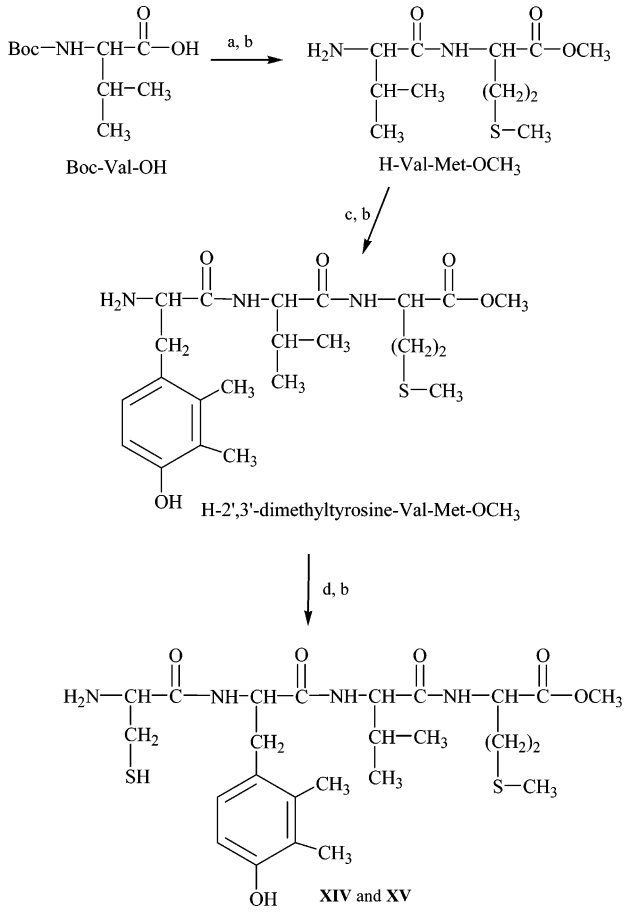

Reagents and conditions: (a) H-Met-OCH_3, WSCD/HOBt/TEA; (b) 4N HCl in dioxane; (c) Boc-D/L-2′,3′-dimethyltyrosine, WSCD/HOBt/TEA; (d) Boc-Cys(Trt)-OH, WSCD/HOBt/TEA

1c−**4c** were reacted with diethyl acetamidomalonate in the presence of EtOH/Na affording the corresponding benzylmalonate derivatives (**1d**−**4d**), which were successively hydrolyzed and decarboxylated by treatment with 6N HCl to give the desired amino acids (**1e**−**4e**). The amino acids (**1e**−**4e**) were treated by Fmoc−OSu in dioxane/water (1/1), in the presence of $NaHCO_3$, to obtain the corresponding Fmoc derivatives (**1f**−**4f**). *N*-Formyl-cysteine was obtained by the formylation of H-Cys(Trt)-OH with formic acid and acetic anydride.[11] The tetrapeptides (**I**−**XIII**) were prepared by solid-phase peptide synthesis on an Fmoc-Met-Wang resin (0.49 mmol/g substitution grade) using a Milligen 9050 peptide synthesizer. Fluorenylmethyloxy-carbonyl (Fmoc) was employed as the α-amino protecting group and 2-(1*H*-benzotriazol-1-yl)-1,1,3,3-tetramethyluronium tetrafluoroborate (TBTU)/1-hydroxy-benzotriazole (HOBt)/*N*-methylmorpholine (NMM) was applied to the coupling reactions. Removal of the *N*-Fmoc group was obtained using 25% piperidine in dimethylformamide (DMF); the cleavage of peptides from the resin was effected using a mixture of trifluoroacetic acid (TFA)/triethylsilane/thioanisole/anisole (90/5/3/2). Peptides **XIV** and **XV** (methyl-ester derivatives) were synthesized, step by step, by the standard solution-phase synthesis outlined in Scheme 2.

1-Ethyl-3-(3′-dimethylaminopropyl)carbodiimide hydrochloride (WSCD)/HOBt/triethylamine (TEA) was applied to the coupling reactions; removal of the *N*-Boc group was obtained using 4N HCl in dioxane.[8a] All of the final compounds, purified by reversed-phase high-performance liquid chromatography (RP-HPLC) to greater than 98% purity, gave satisfactory elemental analyses and were characterized by ESI mass spectrometry. The reference compound, CVFM, was synthesized according to the literature.[8a] All of the conventional amino acids and Oic, employed for the synthesis of compounds **I**−**XV**, belonged to the L series; the uncoded aromatic amino acids, inserted in position A_2, were synthesized as racemic mixtures. The resulting peptides were obtained as diastereoisomeric mixtures that were separated using preparative HPLC because they had different retention times.

The absolute configuration of the unconventional aromatic amino acid units (2′,4′-dimethylphenylalanine, 2′,3′-dimethyltyrosine, 2′,5′-dimethyltyrosine and 2′-dimethyltyrosine) in the diastereomeric couples **II**/**III**, **IV**/**V**, **VI**/**VII**, and **VIII**/**IX** was determined by the application of a nonempirical chromatographic method, referred to as advanced Marfey's method.[12] This method, which relies on the elution order of the amino acids derivatized with (1-fluoro-2,4-dinitrophenyl)-5-L-alaninamide (FDAA), was tested on a series of protein and nonprotein amino acids[13] and invariably, the L-amino acid-FDAA derivative was eluted from a C_{18} column before its corresponding D-isomer. It is well established by NMR and UV measurements that the resolution between L- and D-amino acid derivatives is due to different hydrophobicities, which are derived from the cis- or trans-type arrangements of two more hydrophobic substituents at the α-carbon of the analyzed amino acid and L-Ala-NH_2. Therefore peptides **II**, **V**, **VI**, and **VIII** were subjected under vacuum to vapor-phase hydrolysis to obtain a better recovery of the amino acid derivatives.[14] The hydrolizated peptides and racemic mixtures **1e**, **2e**, **3e**, and **4e** were derivatized with Marfey's reagent (FDAA) and subjected to HPLC analysis. Concerning fraction **4e** (the racemic mixture of 2′,4′-dimethylphenylalanine), the HPLC trace of the FDAA derivatives gave two well-resolved peaks at $t_R = 37.1$ and $t_R = 40.1$ min, whose identity was confirmed by ES/MS (*m*/*z*: 468, 2′,4′-dimethylphenylalanine-FDAA + Na^+). On the basis of the literature precedents,[13] we assumed that the first eluted peak had the L configuration. The presence of a peak at $t_R = 37.1$ min in the HPLC trace of the FDAA derivatives of peptide **II** allowed us to assign the L configuration to the 2′,4′-dimethylphenylalanine unit in the above peptide. The same procedure was applied to the FDAA derivatives of fractions **1e**, **2e**, and **3e** (Experimental Section) that showed, in their HPLC traces, two coupled peaks at $t_R = 57.9$ and $t_R = 65.3$ min (*m*/*z*: 484, 2′,3′-dimethyltyrosine-FDAA + Na^+), at $t_R = 59.6$ and $t_R = 65.4$ min (*m*/*z*: 484, 2′,5′-dimethyltyrosine-FDAA + Na^+), and at $t_R = 54.2$ and $t_R = 60.5$ min (*m*/*z*: 470, 2′-methyltyrosine-FDAA + Na^+), respectively. Comparisons of the HPLC traces of the FDAA derivatives of peptides **V**, **VI**, and **VIII** allowed us to establish the configurations of the two residues of dimethyltyrosine as D and L and the configuration of the methyltyrosine residue as L.

Results and Discussion

Biological Evaluation. The pseudopeptides prepared in this study have been tested for their in vitro FTase-inhibitory activity. Compounds with IC_{50} values lower than 100 μM have also been tested for their ability to inhibit cell proliferation. Compounds **I**−**IX** showed IC_{50} values between 11.4 and 0.1 μM (Table 1).

Compounds **I** (where Phe was replaced with the sterically constrained amino acid Oic), **II** (where Phe was replaced with 2′,4′-L-dimethylphenylalanine), and **VI** (where Phe was replaced with 2′,5′-L-dimethyltyrosine) were found to be as active as CVFM with IC_{50} values of 1.0, 2.2, and 2.5 μM, respectively; compound **IV** (where Phe was replaced with 2′,3′-L-dimethyl-

Table 1. Structures and IC_{50} (μM) ± SD Values of **I**−**XV** and Reference Compound CVFM in FTase Bioassay

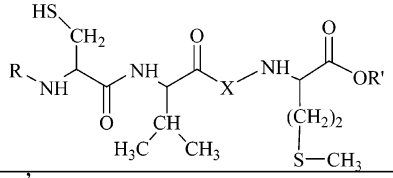

Compound	X	R	R'	IC_{50}	Compound	X	R	R'	IC_{50}
I	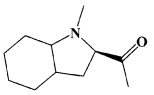	H	H	**1.0±0.9**	**IX**	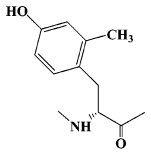	H	H	**11.4±2.6**
II	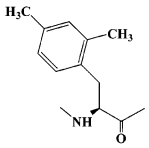	H	H	**2.2±1.4**	**X**	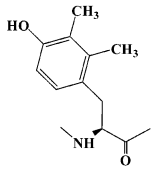	CHO	H	**10.3±3.5**
III	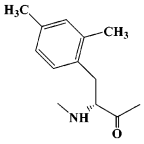	H	H	**4.3±0.8**	**XI**	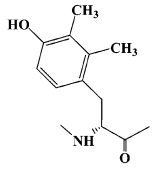	CHO	H	**>100**
IV	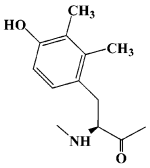	H	H	**0.1±0.07**	**XII**	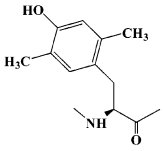	CHO	H	**5.5±3.4**
V	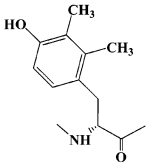	H	H	**4.3±0.6**	**XIII**	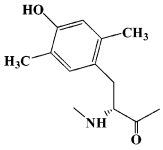	CHO	H	**10.2±2.6**
VI	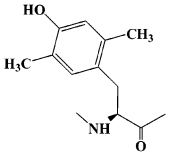	H	H	**2.5±1.4**	**XIV**	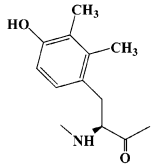	H	CH_3	**20.4±13.3**
VII	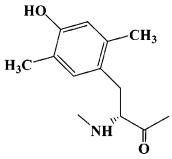	H	H	**10.5±8.2**	**XV**	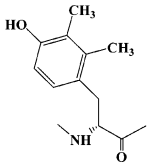	H	CH_3	**70.5±41.3**
VIII	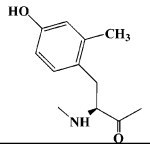	H	H	**4.3±2.1**	**CVFM**	**Phe**	H	H	**0.6±0.2**

tyrosine) is the most active of this series with an IC_{50} value of 0.1 μM (6-fold more active than CVFM). Considering the diastereoisomeric couples, we have verified that in all of the cases compounds containing the L aromatic amino acid were more active than the corresponding diastereisomer incorporating the D enantiomer: compound **II** is 2-fold more active than compound **III**; compound **IV** is 40-fold more active than compound **V**; compound **VI** is 4-fold more active than compound **VII**; and compound **VIII** is about 3-fold more active than compound **IX**. These results could suggest that there is an enantioselective interaction with the enzyme where the L-enantiomer orientation is preferred to the D orientation. Among compounds embodying the tyrosine analogues, those supporting two methyl groups and one −OH group were more active than those supporting just one methyl and one −OH group; peptides **IV** and **VI** and peptides **V** and **VII**, in fact, showed IC_{50} values

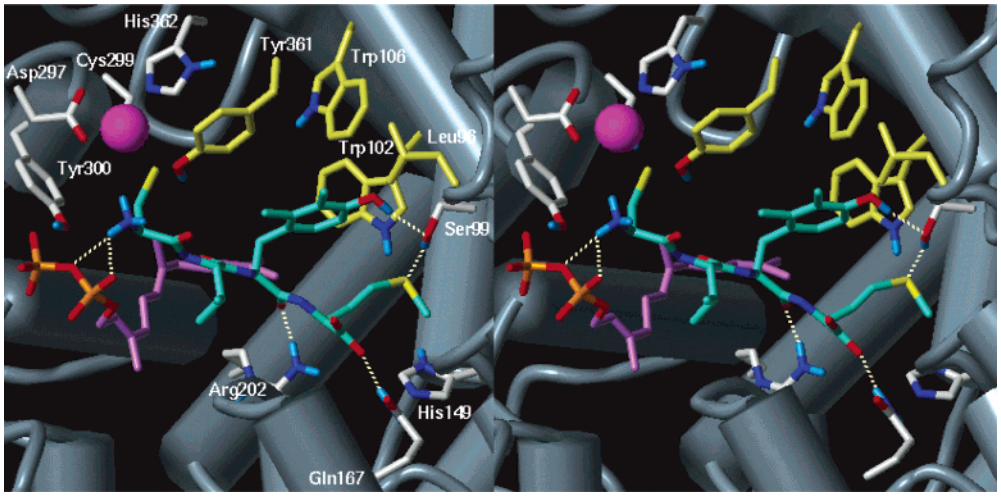

Figure 1. Stereoview of the active site showing FTase inhibitor **IV** (bluishgreen) and the FPP analogue (violet). The protein residues within 4 Å from the docked ligand are shown and labeled. The three aromatic side chains that define a hydrophobic pocket (Trp102, Trp106, and Tyr361) are shown in yellow. The zinc ion is shown as a sphere (magenta). The hydrogen bonds are represented with yellow dashed lines. Nonpolar hydrogen atoms were removed for clarity.

lower than those of **VIII** and **IX**, respectively. Replacement of Phe with 2′,3′-dimethyltyrosine gave the best results (**IV** and **V**); compounds with 2′,5′-dimethyltyrosine (**VI** and **VII**) are, respectively, 25- and 2.5-fold less active than the corresponding 2′,3′-isomer, suggesting the existence of an additional hydrophobic interaction with the enzyme that is stronger when the methyl group is located in the 3′ position. Compounds **I**−**IX**, resulted active from the enzymatic assay, were tested to evaluate whether they were able to inhibit cell proliferation. The pharmacological activity of these compounds were determined in an in vitro assay on a panel of cell lines: FRTL-5, a normal rat-epithelial-thyroid cell line along with a derived clone transformed by v-H-Ras, NIH3T3 mouse embryo fibroblasts, MCF10, a normal human-breast-epithelial cell line, and the human-tumor cell lines MCF7, MDA MB-231, T47D, and LoVo. All of the peptides (**I**−**IX**) did not exhibit any cell-growth inhibition; this disappointing result could be due to the fact that these peptides are not able to penetrate the cell membrane because of their zwitterionic nature. Among many factors that affect the activity of compounds in a cell-based assay, a compound's ability to penetrate the cell membrane is certainly important. For this reason, we decided to synthesize the *N*-formyl and the methyl-ester derivatives of the most active compounds from the enzymatic assay, aiming to facilitate cellular uptake. The newly obtained compounds (**X**−**XV**) were first evaluated in the enzymatic assay against FTase, showing IC_{50} values higher than those reported for the corresponding amino- and carboxy-free parent compounds. As for compounds **I**−**IX**, peptides containing the levo enantiomer of the Tyr-derived unnatural amino acids were found to be more active than those containing the dextro enantiomer. Compound **X** is 10-fold more active than **XI** (IC_{50} = 10.3 and 100 μM, respectively); compound **XII** is ≈2-fold more active than **XIII** (IC_{50} = 5.5 and 10.2 μM, respectively); and compound **XIV** is ≈3-fold more active than compound **XV** (IC_{50} = 20.4 and 70.5 μM, respectively). It is interesting to note that the difference in the activity of compounds **IV**/**V** and **X**/**XI** (**IV** is 40-fold more active than **V** and **X** is 10-fold more active than **XI**) is higher than the other diastereoisomeric couples (**II**−**III**, **VI**−**VII**, **VIII**−**IX**, and **XII**−**XIII**); this could suggest that although the presence of a methyl group in position 3′ is very important in the L-enantiomeric orientation, it could be disturbing when the residue is in the D configuration. *N*-Formylated derivatives (**X**−**XIII**) showed lower IC_{50} values compared with those of the $-NH_2$-free parent compounds (**IV**−**VII**). This modification caused a dramatic loss of affinity when performed on the peptides embodying 2′,3′-dimethyltyrosine. The methyl-ester derivatives, **XIV** and **XV**, showed IC_{50} values of 20.4 and 70.5 μM, respectively. This lower enzymatic affinity is consistent with previous observations that the presence of a free carboxylate at the *C*-terminus is important for a strong inhibition of the enzyme.[7] Nevertheless, compounds **X**−**XV**, tested on cell lines, gave interesting results. Compound **X** inhibited cell growth in two human-breast-cancer cell lines (50% inhibition at 100 μM): MDA MB-231 and T47D. Moreover, this product was not active on MCF10, normal human-breast epithelial cells, suggesting a selective action on tumor cells. It is difficult to justify the lack of activity on the breast-cancer cell line MCF7. Several attempts to correlate FTase activity with cytotoxicity have been reported, but the results obtained are conflicting.[15] Regarding the methyl-ester derivatives, compound **XV** was substantially inactive on all of the tested cell lines; however, compound **XIV** resulted active on all of the human tumor cell lines with IC_{50} values of 65, 83, and 90 μM against MCF7, MDA MB-231, and T47D respectively, and showed the most significant effect on the LoVo cells, with an IC_{50} of 9.1 μM.

Molecular Modeling. To rationalize the above-described results, molecular modeling experiments were carried out. To this end, the X-ray structure of rat FTase in complex with farnesyl pyrophosphate (FPP) and the substrate peptide CVFM (pdb ref code 1JCR) were employed.[4] Compound **IV**, which presents the best inhibition potency (IC_{50} = 0.1 μM), was manually docked into the active site by superimposing it onto the enzyme-bound conformation of the CVFM tetrapeptide.

Figure 1 displays the proposed binding mode into the active site of FTase for **IV**, confirming the good fit of the molecule into the peptide binding site of the enzyme. The peptide binds in an extended conformation and spans the large active-site cavity, contacting both the enzyme side chains and the FPP atom.

The terminal carboxylate of the peptidomimetic participates in hydrogen bonds with Gln167α (NH−O distance = 2.0 Å) similar to those in other peptide substrates.[4,16] The *C*-terminal Met (X position in CA_1A_2X sequence) residue of **IV** binds isosterically (L-isomer) in a hydrophobic specificity pocket made up by Ala98, Ala129, Tyr131, Ala151, and Pro152, where it

forms both van der Waals and electrostatic interactions. In particular, the methionine side chain is oriented in such a way that the thioether can accept a weak hydrogen bond from the Ser99β hydroxyl group (OH−S distance = 2.2 Å).[17] The main chain carbonyl of 2′,3′-dimethyltyrosine (A_2 residue of the CA_1A_2X motif) interacts directly with FTase through a hydrogen bond with the guanidinium group of Arg202β (NH−O distance = 2.0 Å). The 2′,3′-dimethyltyrosine side chain binds isosterically (L-isomer) in the hydrophobic A_2 binding pocket defined by residues Leu96β, Trp102β, Trp106β, Tyr361β, and the third FPP isoprene unit, causing hydrophobic interactions. Particularly, residues Trp102β, Trp106β, and Tyr361β form face-on-face or edge-on-face aromatic-stacking interactions with the 2′,3′-dimethyltyrosine ring. Aromatic-stacking interactions can contribute significantly to ligand-binding energy, and aromatic rings that form interactions with the FTase A_2 binding site appear to be an important component of FTase chemistry.[1,4] Moreover, the extra methyl group at position 3′ of 2′,3′-dimethyltyrosine is properly oriented to make hydrophobic contacts with Leu96β and Trp106β, which easily explains the enhancement in the FTase-inhibitory activity of **IV** with respect to the peptides with the same group in position 2′ (**II**, **VI**, and **VIII**).

Although the A_2 binding pocket is mainly dominated by hydrophobic interactions, a hydrogen bond between the OH hydrogen of Ser99β and the OH oxygen of the 2′,3′-dimethyltyrosine (OH−O distance = 1.9 Å) is also observed, which further contributes to the stabilization of the peptide/FTase complex.

It is important to note that the lower activity of **VIII**, which also has a hydroxyl group at the 4′-position able to form a hydrogen bond with Ser99β, seems to be due to the lack of the extra methyl at position 3′, which is involved in hydrophobic interactions with Leu96β and Trp106β. The Val side chain, corresponding to the A_1 residue of the CA_1A_2X motif, is oriented toward the solvent, which is consistent with the wide variety of residues accommodated at this position in protein and peptide substrates.[18]

The Cys residue of **IV**, which is thought to bind as a thiolate,[19] directly coordinates the catalytic zinc ion at a sulfur−zinc distance of 1.9 Å, whereas its positively charged *N*-terminus forms two ion pairs with O and the phosphate oxygen of the FPP substrate (NH−O distance of 2.5 and 2.2 Å, respectively). According to this, the low inhibitory potency observed for *N*-formyl derivatives **X**−**XIII** seems to be due to the inability of the HCONH-function to form ion pairs with the FPP substrate.

In an effort to elucidate the reasons for the difference in activity observed when comparing the different diastereoisomeric couples, manual superposition of low active compound **V** (D-isomer) on the docked structure of **IV** was carried out. From a visual inspection of the FTase/**V** complex, it seems clear that the extra methyl at the 3′-position of the dimethyltyrosine moiety causes a steric repulsion with the walls of the binding cleft and changes the optimal binding mode of the ligand, thus decreasing the relative stability of the complex. This justifies the lower enantioselectivity observed in diastereoisomeric couples **II**−**III**, **VI**−**VII**, **VIII**−**IX**, and **XII**−**XIII**, which do not possess the 3′-methyl group.

These results suggest the molecular basis of FTase inhibition by **IV**. In particular, this compound inhibits the FTase selectively occupying the binding site of tetrapeptide substrate CVLS, corresponding to the *C*-terminal sequence of the p21 Ras protein, and thus it can be defined as a peptidomimetic inhibitor. The ability to compete with this natural substrate seems to be independent of its capacity to achieve a stable interaction with the Zn^{2+} ion, but it depends on the possibility of forming an ion pair between the peptide *N*-terminus and the α-phosphate of the FPP substrate as well as the stacking interactions and/or H bonds between the 2′,3′-dimethyltyrosine side chain and the FTase A_2 binding site (Figure 2).

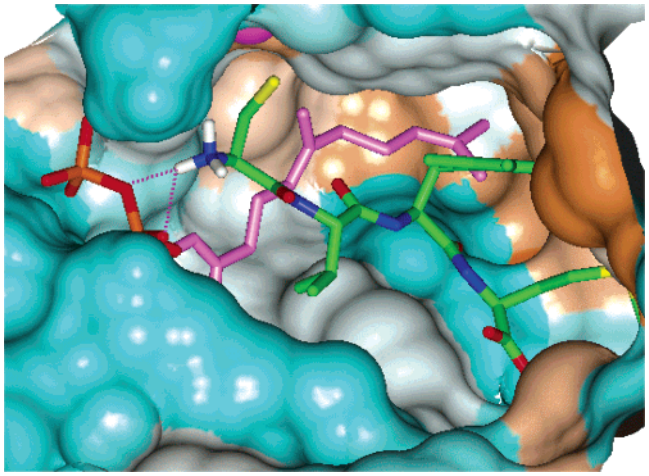

Figure 2. Docking of inhibitor **IV** displayed into the active site of FTase. The molecular surface of the active site has been calculated using the program MOLCAD (implemented in the molecular modeling software package SYBYL). Hydrophobic (brown), neutral (white), and hydrophilic (cyan) properties are displayed on the enzyme's surface. The FPP analogue is displayed in magenta, whereas enzyme-bound zinc is shown as a magenta sphere.

Conclusions

In conclusion, our study describes the synthesis and the pharmacological evaluation of a series of tetrapeptidic compounds containing unconventional amino acids derived from tyrosine and phenylalanine to verify the chance of an additional hydrophobic interaction with the FTase binding site. Molecular modeling studies, carried out on the most potent compound of the series (**IV**, IC_{50} = 0.1 μM), have supported the hypothesis derived from the biological data, suggesting the molecular basis of the FTase inhibition by **IV**. It is clear that the stereochemistry as well as the presence of a hydrophobic group in position 3′ of the aromatic residue A_2 strongly influences the interaction with the FTase binding site. This product, then, can be considered to be a peptidomimetic inhibitor that selectively occupies the binding site of tetrapeptide substrate CVLS, which corresponds to the *C*-terminal sequence of p21 Ras protein.

Experimental Section

Materials and Methods. All solvents were purchased from Carlo Erba (Rodano, Milan, Italy). Extraction solvents were dried over sodium sulfate. The solvents used for the reactions were dried over 3-Å-molecular sieves. All solvents were filtered and degassed prior to use. Reagent grade materials were purchased from Bachem (Bubendorf, Switzerland) and from Aldrich (Milan, Italy) and were used without further purification. Thin-layer chromatography was performed on precoated silica gel Kieselgel 60F254 (E.Merck, A. G.; Darmstadt, Germany) plates. The compounds were detected on thin-layer chromatography plates by UV light and either chlorination followed by a solution of 1% starch-15; KI (1:1, v/v) or ninhydrin. Amino acids analyses were performed in a Carlo Erba 3A-29 amino acid analyzer, and the Cys values were not detected. Molecular weights of final peptides were assessed by electrospray-ionization mass spectrometry (ESI/MS) on a ThermoFinnigan LCQ Ion-Trap. Where analyses are indicated only by the symbols of the elements, results obtained are within ±0.4% of the theoretical values.

The ^{1}H NMR spectra were recorded on a Bruker AM-500 spectrometer. All NMR spectra were obtained in dilute $CDCl_3$ or CD_3OD solutions. Reversed-phase purification was routinely performed on a Waters Delta-Prep 4000 system equipped with a Waters 484 multiwavelength detector on a Vydac C_{18} silica (15−20 μm, 50 × 250 mm) high-performance liquid chromatography (HPLC) column. The operational flow rate was 60 mL/min. The homogeneity of the products was assessed by analytical reversed-phase HPLC using both a Vydac C_{18} column (5 μm, 4.6 × 250 mm) and a Beckman C_{18} column (5 μm, 4.6 × 250 mm) employing the following conditions: eluent A, 0.05% TFA (v/v) in water; eluent B, 0.05% TFA(v/v) in acetonitrile; gradient 0−50% B over 30 min on the Vydac C_{18} column and 5−35% B over 30 min on the Beckman C_{18} column; UV detection at 220 nm, and a flow rate of 1 mL/min. The column was connected to a Rheodyne model 7725 injector, a Waters 600 HPLC system, a Waters 486 tunable absorbance detector set to 220 nm, and a Waters 746 chart recorder.

Amino Acid Synthesis. The unconventional amino acids (**1e**−**4e**) were prepared according to the method of Abrash et al. ad hoc modified and summarized in Scheme 1.[9] Here we report the synthetic procedure and NMR data only for the Fmoc derivatives (**1f**−**2f**) of the unconventional amino acids that were not previously described.

2(*R*/*S*)-(9*H*-Fluoren-9-ylmethoxycarbonylamino)-3-(4-hydroxy-2,3-dimethyl phenyl)-propionic acid (Fmoc-D,L-2′,3′-dimethyltyrosine-OH) (1f). *H*-D,L-2′,3′-Dimethyltyrosine-OH·HCl (**1e**, 1.6 g) was suspended in 25 mL of 9% Na_2CO_3 and cooled in ice water. A solution of 2.4 g of Fmoc−OSu in 25 mL of dioxane was then added dropwise, and the mixture was stirred at room temperature for 3 h. The solvent was evaporated, then ethyl acetate was added, and the water and organic phases were separated. The organic phase was evaporated, and the residue, loaded onto a silica gel column, was purified using diethyl ether−hexane (8:2) as eluent. Fractions containing the product were pooled and concentrated to obtain a white solid: yield 2.3 g (75%). ^{1}H NMR (MeOD) δ: 1.90 (s, 3H), 2.10 (s, 3H), 2.68−2.78 (m, 1H), 3.10−3.21 (m, 1H), 3.79−3.86 (m, 1H), 4.46−4.70 (m, 3H), 6.37−7.84 (m, 10H, aromatic); MS/ESI (+), *m*/*z*: 432 (M + H$^+$). Anal. ($C_{26}H_{25}NO_5$) C, H, N.

Using the procedure described above for the preparation of **1f**, the following additional intermediates were synthesized using, as starting material, unconventional amino acids **2e**, **3e**, and **4e**, respectively:

2(*R*/*S*)-(9*H*-Fluoren-9-ylmethoxycarbonylamino)-3-(4-hydroxy-2,5-dimethylphenyl)-propionic acid (Fmoc-D,L-2′,5′-dimethyltyrosine-OH) (2f). Yield 87%. ^{1}H NMR (MeOD) δ: 2.12 (s, 3H), 2.35 (s, 3H), 3.10−3.13 (m, 1H), 3.29−3.35 (m, 1H), 4.19−4.22 (m, 1H), 4.40−4.60 (m, 3H), 6.37−7.84 (m, 10H, aromatic); MS/ESI (+), *m*/*z*: 432 (M + H$^+$). Anal. ($C_{26}H_{25}NO_5$) C, H, N.

2(*R*/*S*)-(9*H*-Fluoren-9-ylmethoxycarbonylamino)-3-(4-hydroxy-2-methylphenyl)-propionic acid (Fmoc -D,L-2′-methyltyrosine-OH) (3f). Yield 60%. ^{1}H NMR (MeOD) δ: 2.30 (s, 3H), 3.00−3.05 (m, 1H), 3.23−3.27 (m, 1H), 4.10−4.13 (m, 1H), 4.46−4.58 (m, 3H), 6.68−7.84 (m, 11H, aromatic); MS/ESI (+), *m*/*z*: 418 (M + H$^+$). Anal. ($C_{25}H_{23}NO_5$) C, H, N.

2(*R*/*S*)-(9*H*-Fluoren-9-ylmethoxycarbonylamino)-3-(2,4-dimethylphenyl)-propionic acid (Fmoc-D,L-2′,4′-dimethylphenylalanine) (4f). Yield 68%. ^{1}H NMR (MeOD) δ: 2.15 (s, 3H), 2.20 (s, 3H), 3.08−3.10 (m, 1H), 3.25−3.28 (m, 1H), 4.15−4.18 (m, 1H), 4.41−4.73 (m, 3H), 6.81−7.75 (m, 11H, aromatic); MS/ESI (+), *m*/*z*: 416 (M + H$^+$). Anal. ($C_{26}H_{25}NO_4$) C, H, N.

Peptide Synthesis. Compounds **I**−**XIII** were prepared by solid-phase peptide synthesis on a 0.1 mmol scale using an Fmoc-Met-Wang resin (0.49 mmol/g substitution grade) using a Milligen 9050 peptide synthesizer. Fmoc was employed as the α-amino protecting group, and Trt was used as the side-chain protecting group for amino terminal Cys; TBTU/HOBt/NMM was applied to the coupling reactions. *N*-Formyl-cysteine, obtained by the formylation of H-Cys-(Trt)-OH with formic acid and acetic anydride,[11] was employed as the *N*-terminal residue for the synthesis of compounds **X**−**XIII**. The cleavage of the *N*-Fmoc protecting group, using 25% piperidine (v/v) in DMF, was monitored at each stage by measuring the absorbance of the liberated *N*-(9-fluorenylmethyl)piperidine. The complete protected peptide resins were treated with 20 mL of TFA/triethylsilane/thioanisole/anisole (90/5/3/2) at room temperature for 2 h; the mixture was filtered and the resin washed with TFA/CH_2Cl_2 (1:1). The combined filtrate and washings were evaporated and the free peptides, **I**−**XIII**, precipitated with diethyl ether. The crude material, containing the diastereoisomeric couples and several minor impurities as judged by analytical HPLC, were purified by preparative HPLC. Peptides **XIV** and **XV** (methyl-ester derivatives) were synthesized, step by step, by the standard solution-phase synthesis outlined in Scheme 2. The intermediates, obtained using procedures previously reported,[8a] were characterized by ESI/MS, furnishing the expected molecular weights.

Compound **I** and diastereoisomeric couples **II**−**III**, **IV**−**V**, **VI**−**VII**, **VIII**−**IX**, **X**−**XI**, **XII**−**XIII**, and **XIV**−**XV** were purified by reversed-phase HPLC using a two solvent system: A: 0.1% TFA (v/v) in water and B: 0.1% TFA (v/v) in acetonitrile (linear gradient from 0 to 55% B over 60 min, UV detection at 220 nm, and a flow rate of 60 mL/min). The purified peptides were examined for homogeneity by analytical HPLC determinations that were carried out using both a Vydac C_{18} column (5 μm, 4.6 × 250 mm) and a Beckman C_{18} column (5 μm, 4.6 × 250 mm) employing the following conditions: eluent A, 0.05% TFA (v/v) in water; eluent B, 0.05% TFA(v/v) in acetonitrile; gradient 0−50% B over 30 min on the Vydac C_{18} column and 5−35% B over 30 min on the Beckman C_{18} column, UV detection at 220 nm, and a flow rate of 1 mL/min. The final HPLC purity of the peptides was always >98%. The analytical parameters of the purified peptides are listed in Table 2 (Supporting Information).

Determination of Absolute Stereochemistry. (a) General Procedure for Peptide Hydrolysis. Peptide samples (200 μg) were dissolved in degassed 6 N HCl (0.5 mL) in an evacuated glass tube and heated at 160 °C for 16 h. The solvent was removed in vacuo, and the resulting material was subjected to further derivatization. **(b) General Procedure for Obtaining FDAA Derivatives.** A portion of the hydrolyzed mixture (800 μg) or the amino acid enantiomeric mixture (500 μg) was dissolved in 80 μL of a 2:3 solution of TEA−MeCN and treated with 75 μL of 1% *N*-(3-fluoro-4, 6-dinitrophenyl)-L-alaninamide (FDAA) in 1:2 MeCN−acetone. The vials were heated at 70 °C for 1 h, and the contents were neutralized with 0.2 N HCl (50 μL) after cooling to room temperature.

HPLC and Mass Analysis of Marfey's (FDAA) Derivatives. Peptide II and Racemic Amino Acid Mixture 4e. An aliquot of the L-FDAA derivative was dried under vacuum, diluted with MeCN−5% HCOOH in H_2O (1:1), and separated on a Vydac C_{18} (25 × 1.8 mm i.d.) column. A linear gradient (H_2O (0.2% TFA)/acetonitrile (0.1% TFA) (90:10 to 50:50)) over 45 min at 2 mL/min was used, and the FDAA derivatives were detected by UV at 340 nm. Peak identity was confirmed by ESI/MS analysis. The mass spectra were acquired in positive-ion detection mode (*m*/*z* interval of 320−900), and the data was analyzed using the Xcalibur (ThermoQuest, San José, California) suite of programs; all masses were reported as average values. Capillary temperature was set at 280 °C, capillary voltage at 37 V, tube lens offset at 50 V, and ion spray voltage at 5 V. The retention times of authentic FDAA amino acids (min): L-2′,4′-dimethylphenylalanine (37.1) and D-2′,4′-dimethylphenylalanine (40.1). The hydrolyzate of peptide **II** contained L-Met (46.8), l-Val (53.8), and L-2′,4′-dimethylphenylalanine (37.1).

Peptides V, VI, and VIII and Racemic Amino Acid Mixture 1e, 2e, and 3e. To obtain a better resolution in the HPLC traces, the FDAA derivatives were analyzed on a Vydac C_{18} (25 × 1.8 mm i.d.) column by means of a linear gradient from 85 to 15% H_2O (0.2% TFA)/4:1 acetonitrile/2-propanol (0.1% TFA) over 115 min at 1 mL/min (UV detection at 340 nm). Peak identity was also confirmed by ESI/MS analysis.

The retention times of authentic FDAA amino acids (min): L-2′,3′-dimethyltyrosine (57.9), d-2′,3′-dimethyltyrosine (65.3), L-2′,5′-dimethyltyrosine (59.6), D-2′,5′-dimethyltyrosine (65.4), l-3′-methyltyrosine (54.2), and D-2′-methyltyrosine (60.5).

The hydrolyzate of peptide **V** contained: L-Met (46.8), L-Val (53.8), and D-2′,3′-dimethyltyrosine (65.3).

The hydrolyzate of peptide **VI** contained: L-Met (46.8), L-Val (53.8), and L-2′,5′-dimethyltyrosine (59.6).

The hydrolyzate of peptide **VIII** contained: L-Met (46.8), L-Val (53.8), and L-2′-methyltyrosine (54.2).

Computational Chemistry. All molecular modeling was performed using the software package SYBYL[20] running on a Silicon Graphics Octane 2 R12000 workstation. Molecular models of compound **IV** and its derivatives were built according to SYBYL-standard bond lengths and valence angles. Geometry optimizations were realized with the SYBYL/MAXIMIN2 minimizer by applying the BFGS algorithm[21] and setting a root-mean-square gradient of the forces acting on each atom at 0.05 kcal/mol Å as a convergence criterion. Molecular graphics, root-mean-squares (rms) fit, and calculations of ring centroids of substructures were also carried out using SYBYL.

Docking simulations were carried out using the X-ray structure of rat FTase in complex with farnesyl pyrophosphate (FPP) and the substrate peptide CVFM(pdb ref code 1JCR).[4] Water molecules were deleted. Hydrogen atoms were added to the unfilled valences of the amino acids, and the Lys, Asp, and Glu side chains were modeled in their ionized forms.

To build **IV**, the experimentally determined FTase-bound conformation of CVFM was modified by replacing the phenylalanine residue with the 2′,3′-dimethyltyrosine side chain. Hydrogen atoms were added to the unfilled valences and their positions optimized while keeping the rest of the molecule fixed.

The position of the docked tetrapeptide CVFM in the enzyme crystal structure was taken as a starting point. Peptide **IV** was docked into the FTase binding site by means of the following steps: (i) superposition on the enzyme-bound conformation of CVFM by minimizing the root-mean-square distance between their common backbone atoms; (ii) removal of CVFM from the receptor; (iii) manual adjustment of the torsion angles determining the orientation of the 2′,3′-dimethyltyrosine side chain of **IV** to avoid steric clashes with the enzyme; and (iv) energy-minimization of the resulting **IV**/FTase complex on the basis of the molecular mechanics Tripos force field.[22] During the minimization step, the side chains and the ligand itself were allowed to optimize their position and conformation by keeping the protein backbone atoms fixed.

Biological Assays. Farnesyltransferase Protein. The enzyme was a partially purified fraction from a bovine brain homogenate, prepared essentially as described by Reiss et al.[23]

Farnesyltransferase Inhibition Assay. To evaluate the farnesyltransferase inhibition by our compounds, we have used Amersham's farnesyl transferase kit based on the scintillation proximity principle. A human lamin-B carboxy-terminus sequence peptide (biotin-YRASNRSCAIM) is ^{3}H-farnesylated at the cysteine residue when processed by farnesyl transferase. The resultant complex is captured by streptavidin-linked SPA beads. In a 100 μL final reaction volume, the test compound was added in 10 μL of DMSO to a 70 μL reaction mixture containing 20 μL of 1:20 diluted [^{3}H]-farnesyl pyrophosphate (0.2 μCi), 46 μL of assay buffer (50 mM HEPES, 30 mM $MgCl_2$, 20 mM KCl, 5 mM DTT, and 0.01% Triton X-100), and 20 μL of 0.5 mM biotin-lamin B peptide in a buffer at pH 7.5 (50 mM HEPES, 25 mM Na_2HPO_4, 20 mM KCl, 5 mM DTT, and 0.01% Triton X-100). This mixture was allowed to stand at 37 °C for 5 min. The reaction was started by adding 4 μL of diluted enzyme ($\sim$2 μg of protein) to the mixture that was incubated at 37 °C for 1 h. To stop the reaction, 150 μL of the stop/bead reagent was added. The samples were counted in a Beckman LS 1801 scintillation counter. Every test compound was assayed at least twice, and the mean and standard deviation were calculated.

Cell Lines. FRTL-5 is a continuous line of differentiated epithelial cells derived from normal Fisher rat thyroid that have retained the typical markers of thyroid differentiation such as thyroglobulin (TG), thyroperoxidase (TPO), and thyrotropin receptor (TSH-R) and depend for growth upon the continuous presence of thyroid stimulating hormone (TSH) in the medium. In vitro experiments on FRTL-5 rat thyroid cells have shown that v-H-Ras is able, in a single step, to malignantly transform this cell line.[24]

The FRTL-5 cells were grown in Coon's modified Ham F12 medium supplemented with 5% calf serum and a mixture of six hormones: TSH 1×10^{-10} M, insulin 10 mg/mL, somatostatin 10 ng/mL, Glycyl-Histidyl-Lysine acetate 10ng/mL, hydrocortisone 1×10^{-8} M, and transferrin 5 mg/mL. FRTL-5 cells fully transformed by the v-H-Ras oncogene were grown in Coon's modified Ham F12 medium supplemented with 5% calf serum.

NIH 3T3 mouse embryo fibroblasts were grown in DMEM medium with 10% calf serum. The normal breast-epithelial cells MCF10 were cultured in 1:1 DMEM/Ham's-F12 medium (Life Technologies, Inc.) with 5% horse serum supplemented with 20 ng/mL EGF, 100ng/mL cholera toxin, 0.01 bovine insulin, and 500 ng/mL hydrocortisone. Human tumor cell lines MCF7, T47D, and MDA MB-231 derived from breast carcinomas and LoVo from a colon carcinoma were all grown as monolayers in RPMI-1640 (Life Technologies, Inc., NY) containing 10% fetal bovine serum (Life Technologies, Inc., NY).

Compound Treatment. Cells were grown in a volume of 100 μL at approximately 10% confluency in 96-well multititer plates and were allowed to attach and recover for another 24 h. Varying concentrations of compounds alone were then added to each well, and the plates were incubated in an atmosphere of 5% CO_2 and 95% air at 37 °C for an additional 24 h. Finally, the plates were washed to remove the drug and incubated for 48 h. The control cultures included equivalent amounts of the vehicle used to solubilize each molecule. The experimental agents were solubilized in DMSO.

Sulforhodamine B Assay. At the end of the treatment, cell viability was assessed by the sulforhodamine B (SRB) assay.[25] Data were expressed as %T/C = (OD of treated cells/OD of control cells) $\times$ 100, and the concentration of the test compound causing 50% inhibition of cell growth (IC_{50}) was calculated from the dose/effect curve for each tested compound. Every assay was performed in triplicate, and the drug-IC_{50} value of each cell line was the average of at least three independent experiments.

Acknowledgment. This work was supported by the Italian MIUR fund (PRIN 2005).

Supporting Information Available: Analytical data (Table 2) and elemental analysis (Table 3) for all compounds. This material is available free of charge via the Internet at http://pubs.acs.org.

References

(1) Reid, S. T.; Beese L. S.. Crystal structures of the anticancer clinical candidates R115777 (Tipifarnib) and BMS-214662 complexed with protein farnesyltransferase suggest a mechanism of FTI selectivity. *Biochemistry*, **2004**, *43*, 6877−6884.

(2) El Oualid, F.; Burm, B. E. A.; Leroy, I. M.; Cohen, L. H.; van Boom, J. H.; van den Elst, H.; Overkleeft, H. S.; van der Marel, G. A.; Overhand, M. Design, synthesis, and evaluation of sugar amino acid based inhibitors of protein prenyl transferases PFT and PGGT-1. *J. Med. Chem.* **2004**, *47*, 3920−3923.

(3) Brunner, T. B.; Hahn, S. M.; Gupta, A. K.; Muschel, R. J.; McKenna, W. G.; Bernhard, E. J. Farnesyltransferase inhibitors: an overview of the results of preclinical and clinical investigations. *Cancer Res.* **2003**, *63*, 5656−5668.

(4) Long, S. B.; Hancock, P. J.; Kral, A. M.; Hellinga, H. W.; Beese, L. S. The crystal structure of human protein farnesyltransferase reveals the structural basis for inhibition by CaaX tetrapeptides and their mimetics. *Proc. Natl. Acad. Sci. U.S.A.* **2001**, *98*, 12948−12953.

(5) Bell, I. M. Inhibitors of farnesyltransferase: a rational approach to cancer chemotherapy? *J. Med. Chem.* **2004**, *47*, 1869−1878.

(6) Leftheris, K.; Kline, T.; Natarajan, S.; DeVirgilio, M. K.; Cho, Y. H.; Pluscec, J.; Ricca, C.; Robinson, S. Peptide based $P21^{RAS}$ farnesyl transferase inhibitors: systematic modification of the tetrapeptide CA_1A_2X motif. *Bioorg. Med. Chem. Lett.* **1994**, *4*, 887−892.

(7) Lee, H. Y.; Sohn, J. H.; Kwon, B. M. Development of tripeptidyl farnesyltransferase inhibitors. *Bioorg. Med. Chem. Lett.* **2002**, *12*, 1599−1602.

(8) (a) Caliendo, G.; Fiorino, F.; Grieco, P.; Perissutti, E.; Santagada, V.; Ramunno, A.; Albrizio, S.; Califano, D.; Giuliano, A.; Santelli, G. Phenol-derived CVFM analog inhibitors of Ras Farnesyltransferase possessing cellular in vitro activity *Eur. J. Med. Chem*. **1998**, *33*, 725−732. (b) Caliendo, G.; Fiorino, F.; Grieco, P.; Perissutti, E.; De Luca, S.; Giuliano, A.; Santelli, G.; Califano, D.; Severino, B.; Santagada, V. Synthesis and biological activity of pseudopeptides inhibitors of Ras farnesyl transferase containing unconventional amino acids. *Farmaco*, **1999**, *54*, 785−790.

(9) Santagada, V.; Caliendo, G.; Severino, B.; Perissutti, E.; Ceccarelli, F.; Giusti, L.; Mazzoni, M. R.; Salvadori, S.; Temussi, P. A. Probing the shape of a hydrophobic pocket in the active site of delta-opioid antagonists. *J. Pept. Sci*. **2001**, 7, 374−385.

(10) (a) Vincent, M.; Remond, G.; Portevin, B.; Serkiz, B.; Laubie, M. Stereoselective synthesis of a new perhydroindole derivative of chiral iminodiacid, a potent inhibitor of angiotensin converting enzyme. *Tetrahedron Lett*. **1982**, *23*, 1677−1680.

(11) Sheehan, J. C.; Yang, D. D. H. The use of *N*-formylamino acids in peptide synthesis. *J. Am. Chem. Soc.* **1958**, *80*, 1154−1158.

(12) (a) Harada, K.; Fujii, K.; Mayumi, T.; Hibino, Y.; Suzuki, M. A method using LC/MS for determination of absolute configuration of constituent amino acids in peptide advanced Marfey's method. *Tetrahedron Lett.* **1995**, *36*, 1515−1518. (b) Fujii, K.; Ikai, Y.; Mayumi, T.; Oka, H.; Suzuki, M.; Harada, K. A nonempirical method using LC/MS for determination of the absolute configuration of constituent amino acids in a peptide: elucidation of limitations of Marfey's method and of its separation mechanism. *Anal. Chem*. **1997**, *69*, 3346−3352.

(13) Péter, A.; Olajos, E.; Casimir, R.; Tourwé, D.; Broxterman, Q. B.; Kaptein, B.; Armstrong, D. W. High-performance liquid chromatographic separation of the enantiomers of unusual amino acid analogues. *J. Chromatogr., A* **2000**, *871*, 105−113.

(14) Davidson, I. Protein Sequencing Protocol. In *Methods in Molecular Biology*, 2nd ed.; Smith, B. J., Ed.; Humana Press: Totowa, NJ, ; Vol. 211.

(15) (a) Smith, V.; Rowlands, M. G.; Barrie, E.; Workman, P.; Kelland, L. R. Establishment and characterization of acquired resistance to the farnesyl protein transferase inhibitor R115777 in a human colon cancer cell line. *Clin. Cancer Res*. **2002**, 8, 2002−2009. (b) Moasser, M. M.; Rosen, N. The use of molecular markers in farnesyltransferase inhibitor (FTI) therapy of breast cancer. *Breast Cancer Res. Treat*. **2002**, *73*, 135−144.

(16) (a) Strickland, C. L.; Windsor, W. T.; Syto, R.; Wang, L.; Bond, R.; Wu, R.; Schwartz, J.; Le, H. V.; Beese, L. S.; Weber, P. C. Crystal structure of farnesyl protein transferase complexed with a CaaX peptide and farnesyl diphosphate analogue. *Biochemistry* **1998**, *37*, 16601−16611. (b) Long, S. B.; Casey, P. J.; Beese, L. S. The basis for K-Ras4B binding specificity to protein farnesyltransferase revealed by 2 Å resolution ternary complex structures. *Structure* **2000**, *8*, 209−222.

(17) Desiraju, G. R.; Steiner, T. *Monographs on Crystallography;* Oxford University Press/International Union of Crystallography: Oxford, 1999; Vol. 9.

(18) Reiss, Y.; Stradley, S. J.; Gierasch, L. M.; Brown, M. S.; Goldstein, J. L. Sequence requirement for peptide recognition by rat brain p21Ras protein farnesyltransferase. *Proc. Natl. Acad. Sci. U.S.A.* **1991**, *88*, 732−736.

(19) Hightower, K. E.; Huang, C.-C.; Casey, P. J.; Fierke, C. A. H-Ras peptide and protein substrates bind protein farnesyltransferase as an ionized thiolate. *Biochemistry*, **1999**, *37*, 15555−15562.

(20) *SYBYL Molecular Modeling System*, version 6.9.1; Tripos Inc.: St. Louis, MO, 2003.

(21) Head, J.; Zerner, M. C. A Broyden-Fletcher-Goldfarb-Shannon optimization procedure for molecular geometries. *Chem. Phys. Lett.* **1985**, *122*, 264−274.

(22) Vinter, J. G.; Davis, A.; Saunders, M. R. Strategic Approaches to Drug Design. 1. An integrated software framework for molecular modeling. *J. Comput.-Aided Mol. Des.* **1987**, *1*, 31−55.

(23) Reiss, Y.; Goldstein, J. L.; Seabra, M. C.; Casey, P. J.; Brown, M. S. Inhibition of purified p21Ras farnesyl protein transferase by Cys-AAX tetrapeptides. *Cell* **1990**, *62*, 81−88.

(24) Fusco, A.; Berlingieri, M. T.; Di Fiore, P. P.; Portella, G.; Grieco, M.; Vecchio, G. One- and two-step transformations of rat thyroid epithelial cells by retroviral oncogenes. *Mol. Cell. Biol.* **1987**, *7*, 3365−3370.

(25) Skehan, P.; Storeng, R.; Scudiero, D.; Monks, A.; McMahon, J.; Vistica, D.; Warren, J. T.; Bokesch, H.; Kenney, S.; Boyd, M. R. New colorimetric cytotoxicity assay for anticancer-drug screening. *J. Natl. Cancer Inst.* **1990**, *82*, 1107−1112.

JM0506165